Early-Transition-Metal Macrocycles as Metalloligands: Synthesis and Structure of Dinuclear Zirconocene Thioglycolates $[Cp^\circ_2Zr\{OOC(CH_2SCH_2)_nCOO\}_2ZrCp^\circ_2]$ ($n = 1, 2$) and Their Heterobimetallic Complexes with Mo^0 and Pd^{II} [‡]

Barbara Wenzel, Peter Lönnecke,[†] and Evamarie Hey-Hawkins*

Institut für Anorganische Chemie der Universität Leipzig, Johannisallee 29, D-04103 Leipzig, Germany

Received December 4, 2001

The reactions of $[Cp^\circ_2ZrMe_2]$ ($Cp^\circ = C_5EtMe_4$) with the thioglycolic acids $HOOC(CH_2SCH_2)_nCOOH$ ($n = 1, 2$) resulted in evolution of methane and formation of the macrocyclic, dimeric zirconocene complexes $[Cp^\circ_2Zr(OOCCH_2SCH_2COO)_2ZrCp^\circ_2]$ (**1**) and $[Cp^\circ_2Zr(OOCCH_2SCH_2CH_2SCH_2COO)_2ZrCp^\circ_2]$ (**2**), which can act as metalloligands toward complex fragments of a second metal. Both complexes were characterized by NMR and IR spectroscopy, ESI mass spectrometry, and X-ray diffraction analysis. In solution at room temperature both complexes are dynamic, and the carboxylato groups alternate between mono- and bidentate bonding modes. For complex **1** the free energy of activation for this process was determined to be $\Delta G^\ddagger = 37 \pm 1$ kJ/mol by variable-temperature NMR experiments. Compound **1** reacts with $[Mo(CO)_4(NBD)]$ (NBD = norbornadiene) to give the tetranuclear Zr/Mo complex **3**, the crystal structure of which showed that an $Mo(CO)_4$ fragment is coordinated to one S and one O donor center of each bridging ligand of **1**. This heterobimetallic complex **3** was also characterized by NMR and IR spectroscopy, and in contrast to **1**, it is not dynamic in solution at room temperature, owing to the coordination of the $Mo(CO)_4$ fragments. Compounds **1** and **2** also react with $[PdCl_2(CH_3CN)_2]$ to give the trinuclear Zr/Pd complex **4** and the tetranuclear Zr/Pd complex **5**. Both complexes were characterized by NMR and IR spectroscopy and by elemental analysis.

Introduction

Research on early/late heterobimetallics (ELHBs) has grown in the past few years and has been subject of numerous reports.[1−4] The reasons for this interest include their relevance to bimetallic bioinorganic systems and their potential in homogeneous catalysis. The pairing of two electronically different metals in a single compound may lead to cooperative interactions between the metals, such as those observed in heterogeneous catalysis, and there is also the possibility of stereo- or regioselective catalysis. Heterogeneous catalysts in which late transition metals are dispersed on a Lewis acid support (TiO_2 or Al_2O_3) often show increased catalytic activity.[5−9] Such strong metal−support interactions (SMSI) are not well understood but have been attributed to electronic communication between and cooperative activation of substrates by the different metal centers.[10,11]

For the synthesis of related homogeneous systems we have used an early-transition-metal complex of a bifunctional ligand as a metalloligand for a late transition metal. To date, various bifunctional ligands, for example, S/P,[12,13] S/S,[14−16] S/N,[17] O/P,[18] and N/N,[19,20] have been employed. Due to the different electronic properties of the two metals we used ligands with electronically different O and S donor centers (Pearson's HSAB concept).[21] Thus, we synthesized heterobimetallic complexes in which Zr and Ni or Zr and Pd are bridged by

---

[‡] Dedicated to Professor Dr. Walter Siebert on the occasion of his 65th birthday.

[†] Crystal structure determinations.

(1) Stephan, D. W. *Coord. Chem. Rev.* **1989**, *95*, 42.

(2) Wark, T. A.; Stephan, D. W. *Organometallics* **1989**, *8*, 2836.

(3) Kalck, P.; Serra, C.; Machet, C.; Broussier, R.; Gautheron, B.; Delmas, G.; Trouve, G.; Kubicki, M. *Organometallics* **1993**, *12*, 1021.

(4) Schneider, A.; Gade, L. H.; Breuning, M.; Bringmann, G.; Scowen, I. J.; McPartlin, M. *Organometallics* **1998**, *17*, 1643.

(5) Naito, S. *J. Chem. Soc., Chem. Commun.* **1985**, 1212.

(6) Sinfelt, J. H. *Sci. Am.* **1985**, *235*, 90.

(7) Whyte, T. E.; Dalla Betta, R. A. *Catal. Rev.-Sci. Eng.* **1982**, *24*, 567.

(8) Bell, A. T. *Catal. Rev.-Sci. Eng.* **1981**, *23*, 203.

(9) Maxwell, I. E. *Adv. Catal.* **1981**, *30*, 1.

(10) *Metal Support Interactions in Catalysis, Sintering and Redispersion*; Stephenson, S. A., Dumesic, J. A., Baker, R. T. K., Ruckenstein, E., Eds.; Van Nostrand Reinhold: New York, 1987.

(11) *Strong Metal Support Interactions;* Baker, R. T. K., Tauster, S. J., Dumesic, J. A., Eds.: American Chemical Society: Washington, DC, 1986.

(12) White, G. S.; Stephan, D. W. *Inorg. Chem.* **1985**, *24*, 1499.

(13) White, G. S.; Stephan, D. W. *Organometallics* **1988**, *7*, 903.

(14) Nadasdi, T. T.; Stephan, D. W. *Organometallics* **1992**, *11*, 116.

(15) Stephan, D. W. *Organometallics* **1991,** *10*, 2037.

(16) Boormann, P. M.; Gavin, G. K. W.; Parvez, M. *Polyhedron* **1992**, *11*, 765.

(17) Junghwan, Y.; Jaejung, K.; Sang-Eun, P. *Bull. Kor. Chem. Soc.* **1994**, *15*, 803.

(18) Ferguson, G. S.; Wolczanski, P. T. *Organometallics* **1985**, *4*, 1601.

(19) Sharma, K.; Joshi, S. C.; Singh, R. V. *Met.-Based Drugs* **2000**, *7*, 105.

(20) Sharma, K.; Fahmi, N.; Singh, R. V. *Indian J. Chem.* **1999**, *A38*, 1291.

10.1021/om0110336 CCC: $22.00

Scheme 1

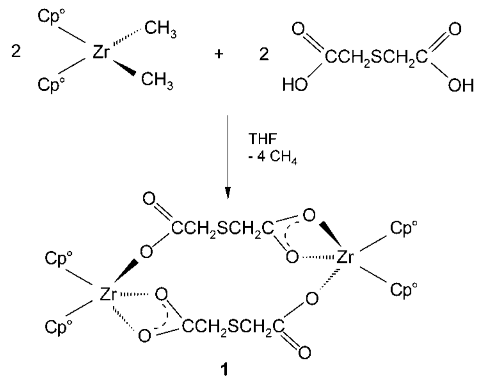

Scheme 2

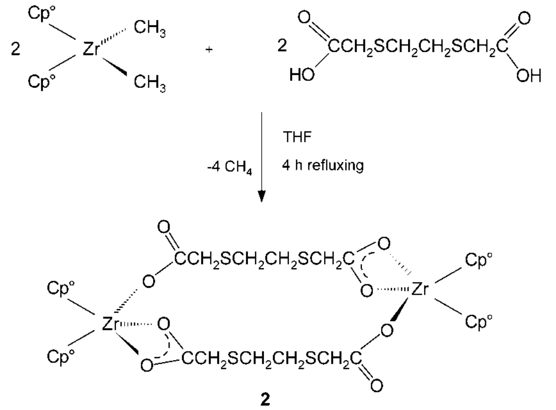

the dianion of mercaptoacetic acid.[22] In this case a monomeric zirconocene mercaptocarboxylato complex acted as the metalloligand, and the late transition metals (Ni, Pd) were coordinated by H abstraction from the SH groups of the ligands. In the present study, we used thioglycolates to obtain dimeric, macrocyclic zirconocene complexes that coordinate the late transition metal at the free sulfur atoms by substitution of labile ligands. Other macrocyclic zirconocene and titanocene complexes with dithiolates[14,15] and dialkoxides[23] as bridging ligands have been reported. The dithiolate macrocycles were used as metalloligands for the synthesis of Zr/Ag,[15] Ti/Cu, and Ti/Ag[14] heterobimetallic complexes. Here we report on the synthesis and structures of the first dimeric, macrocyclic zirconocene thioglycolate complexes and further demonstrate their ability to act as metalloligands for the complexation of molybdenum and palladium.

Results and Discussion

[$Cp°_2Zr(OOCCH_2SCH_2COO)_2ZrCp°_2$] (1) and [$Cp°_2Zr(OOCCH_2SCH_2CH_2SCH_2COO)_2ZrCp°_2$] (2). The dimeric complexes **1** and **2** were obtained by the reaction of [$Cp°_2ZrMe_2$] (Cp° = C_5EtMe_4) with thiodiglycolic or dithiotriglycolic acid in a molar ratio of 1:1 (Schemes 1 and 2). Even when a molar ratio of 1:2 ([$Cp°_2ZrMe_2$]:thiodiglycolic acid) was used in an attempt to obtain a monomeric complex, only the more stable dimeric complex **1** was formed. In contrast to the case for **1**, refluxing the solution for about 4 h is important for obtaining good yields of **2**, because at room temperature the formation of a second compound, presumably the monomeric chelate complex, was observed. The highly substituted cyclopentadienyl ligands are responsible for the solubility of **1** in common organic solvents such as THF and toluene.

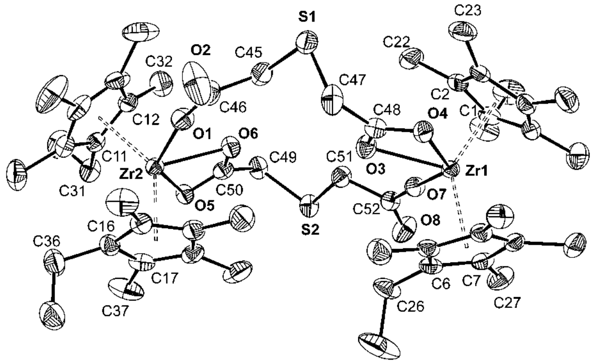

Figure 1. ORTEP plot of **1** (50% thermal ellipsoids are shown; hydrogen atoms are omitted for clarity).

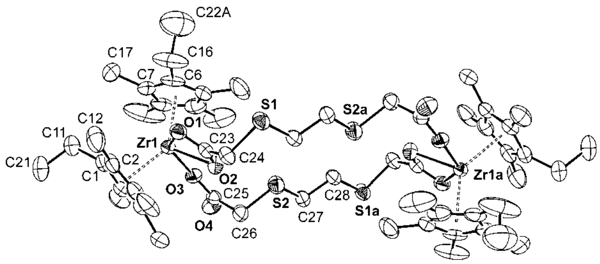

Figure 2. ORTEP plot of **2** (50% thermal ellipsoids are shown; hydrogen atoms are omitted for clarity): (A) disordered atoms; (a) atoms produced by symmetry operation.

Table 1. Selected Bond Lengths (Å) and Angles (deg) for 1

Zr1−O3	2.274(2)	C46−O1	1.285(4)
Zr1−O4	2.286(2)	C46−O2	1.208(4)
Zr1−O7	2.073(2)	C48−O3	1.269(4)
Zr2−O1	2.065(2)	C48−O4	1.263(4)
Zr2−O5	2.296(2)	C50−O5	1.265(4)
Zr2−O6	2.264(2)	C50−O6	1.268(4)
		C52−O7	1.294(4)
		C52−O8	1.210(4)
O3−Zr1−O4	56.83(8)	O3−C48−O4	118.0(3)
O5−Zr2−O6	56.88(8)	O5−C50−O6	118.0(3)
O1−C46−O2	123.9(4)	O7−C52−O8	125.1(5)

Table 2. Selected Bond Lengths (Å) and Angles (deg) for 2

Zr1−O1	2.297(6)	C23−O1	1.262(10)
Zr1−O2	2.275(6)	C23−O2	1.266(10)
Zr1−O3	2.068(6)	C25−O3	1.299(10)
		C25−O4	1.222(11)
O1−Zr1−O2	56.7(2)	O1−C23−O2	118.3(8)
O2−Zr1−O3	78.0(2)	O3−C25−O4	122.6(9)

Structural Studies on 1 and 2. ORTEP plots of **1** and **2** are shown in Figures 1 and 2, and selected bond lengths and angles are given in Tables 1 and 2. Crystal data and data collection parameters are given in Table 4. For **2**, all crystals which were tested for the X-ray measurement were twinned, and this is reflected in the *R* values. In **1** and **2**, both Zr atoms are coordinated by

---

[21] Chattaraj, P. K.; Lee, H.; Parr, R. G. *J. Am. Chem. Soc.* **1991**, *113*, 1855.

[22] Wenzel, B.; Lönnecke, P.; Stender, M.; Hey-Hawkins, E. *J. Chem. Soc. Dalton Trans.* **2002**, 478.

[23] Stephan, D. W. *Organometallics* **1990**, *9*, 2718.

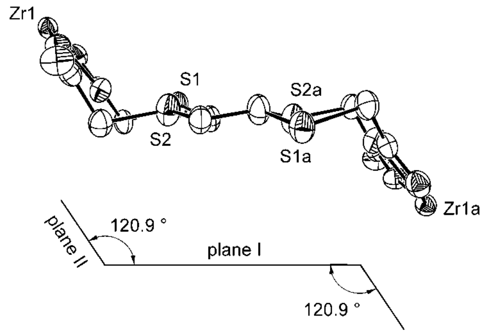

Figure 3. Chair conformation of **2**.

two η^5-cyclopentadienyl rings, as well as one monodentate and one bidentate carboxylato group, so that the Zr atoms each have 18 valence electrons. This bonding mode was also observed in related zirconocene bis(carboxylates)[24−26] and was also described for quite similar dimeric zirconocene furandicarboxylato and isophthalato complexes.[27] The Zr−O bond lengths and O−Zr−O bond angles are comparable to those in known zirconocene dicarboxylates. In **1**, both Zr atoms and the thiodiacetato ligands form a 16-membered ring which, in contrast to that in the isophthalato complex, is nonplanar. In **2**, the zirconium atoms and the bridging ligands form a 22-membered ring, but of greater interest is their arrangement in a chair conformation (Figure 3). S1, S2, C24, C26, C27, and C28 form plane I with a maximum deviation of 0.184(6) Å, and Zr1, O1, O2, O3, O4, C23, and C24 form plane II with a maximum deviation of 0.058(6) Å. The angle between these calculated planes is 120.9(5)°.

Spectroscopic Studies on 1 and 2. In accordance with the crystal structure of **1** and **2**, the IR spectra also show the presence of mono- and bidentate ligands in the solid state. The C=O and C−O stretching bands for the monodentate carboxylato group are observed at $\tilde{\nu}_{C=O}$ 1648 (**1**) and 1635 cm^{-1} (**2**) and $\tilde{\nu}_{C-O}$ 1207 (**1**) and 1205 cm^{-1} (**2**) (in the literature these are often referred to as asymmetric and symmetric vibrations, but in our opinion this is not correct, because the monodentate carboxylato group is not symmetrical, and an ideal coupling of the vibrations is therefore unfavorable). The absorption bands for the asymmetric and symmetric stretches of the bidentate carboxylato group appear at $\tilde{\nu}_{as}$ 1535 cm^{-1} and $\tilde{\nu}_{s}$ 1334 cm^{-1} (for **1**) and 1538 and 1324 cm^{-1} (for **2**).

In the ^{1}H NMR spectrum of **1** the CH_2 groups of the two ligands were observed as a singlet at 3.58 ppm. In the ^{1}H NMR spectrum of **2**, a singlet at 3.32 ppm for the CH_2 groups next to the carboxylato group and a singlet at 3.01 ppm for the ethylene CH_2 groups were observed. The NMR data suggest a rapid dynamic process in which both ligands alternate between mono- and bidentate bonding. Such dynamics were observed for most zirconocene dicarboxylates (see above) and in a zirconocene mercaptoacetate.[22] So far it has not been possible to freeze out this motion at low temperature and to determine the free energy of activation of such a process. We carried out low-temperature NMR experiments on **1** in CD_2Cl_2 and observed splitting of the signals for the CH_2 groups of the thiodiacetato ligands (coalescence temperature T_c = 197 K). By using the modified Eyring equation[28] we determined a free energy of activation of $\Delta G^{\ddagger} = 37 \pm 1$ kJ/mol for this dynamic process. Low-temperature NMR experiments for **2** down to −70 °C failed to freeze out this dynamic process, and we only observed slight broadening of the signals. Thus, **2** shows a higher conformational flexibility in solution than **1**.

Scheme 3

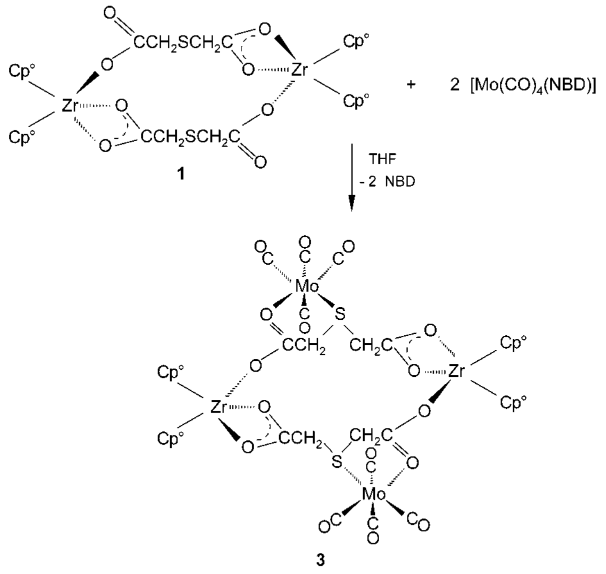

Reaction of 1 with [Mo(CO)$_4$(NBD)]. The dimeric macrocyclic complex **1** reacts with 2 equiv of [Mo(CO)$_4$(NBD)] (NBD = norbornadiene) to give the yellow tetranuclear Zr/Mo complex **3** (Scheme 3). Using a molar ratio of 1:1 also resulted in formation of **3**.

Structural Studies on 3. An ORTEP plot of **3** is shown in Figure 4, and selected bond lengths and angles are given in Table 3. The two Mo(CO)$_4$ fragments are each coordinated to one sulfur and one oxygen donor, and both Mo atoms show a distorted-octahedral coordination sphere. Mo1, S1, O2, O7, C29, and C30 lie in a plane with a maximum deviation for S1 of 0.075(2) Å. The axial CO groups are not exactly perpendicular to this plane (C27−Mo1−C28 = 171.7(2)°), owing to interactions with the bulky Cp° ligands. The coordination of the oxygen atom to molybdenum results in slight π-electron delocalization in the carboxylato groups, which is reflected in the O1−C23 and O2−C23 bond lengths of 1.272(5) and 1.227(5) Å. In a CCDC search we found only two complexes with a Mo coordination sphere similar to that of **3**: [NMe$_4$][Mo(CO)$_4$(SC$_6$H$_4$-SMe)][29] and [Mo(CO)$_4$(PPh$_2$CH$_2$CH$_2$SMe)].[30] The Mo−S bond length of 2.573(1) Å is comparable to that in the phosphinothioether complex. However, of more interest are the Mo−C bond lengths Mo1−C29 trans to O1 and

---

[24] Howard, W. A.; Trnka, T. M.; Waters, M.; Parkin, G. *J. Organomet. Chem.* **1997**, *528*, 95.

[25] Thewalt, U.; Güthner, T. *J. Organomet. Chem.* **1989**, *361*, 309.

[26] Gau, H.-M.; Chen, C.-T.; Jong, T.-T.; Chien, M.-Y. *J. Organomet. Chem.* **1993**, *448*, 99.

[27] Niemann, U.; Diebold, J.; Troll, C.; Rief, U.; Brintzinger, H.-H. *J. Organomet. Chem.* **1993**, *456*, 195.

[28] Hesse, M.; Meier, H.; Zeeh, B. *Spektroskopische Methoden in der organischen Chemie*; Georg Thieme Verlag: Stuttgart, Germany, 1995.

[29] Sellmann, D.; Binker, G.; Schwarz, J.; Knoch, F. *J. Organomet. Chem.* **1987**, *323*, 323.

[30] Adams, R. D.; Blankenship, C.; Segmüller, B. E.; Shiralian, M. *J. Am. Chem. Soc.* **1983**, *105*, 4319.

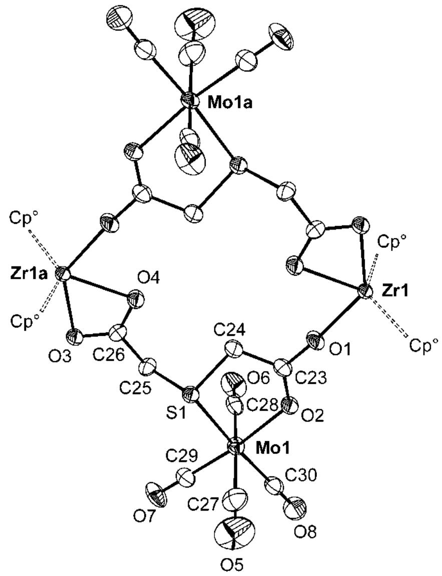

Figure 4. ORTEP plot of **3** (50% thermal ellipsoids are shown; Cp° ligand ellipsoids and hydrogen atoms are omitted for clarity): (a) atoms produced by symmetry operation.

Table 3. Selected Bond Lengths (Å) and Angles (deg) for 3

Zr1−O1	2.100(3)	O1−C23	1.272(5)
Zr1−O3a	2.283(3)	O2−C23	1.227(5)
Zr1−O4a	2.295(3)	O3−C26	1.248(4)
Mo1−S1	2.573(1)	O4−C26	1.269(5)
Mo1−O2	2.252(3)	O5−C27	1.130(6)
Mo1−C27	2.058(6)	O6−C28	1.134(5)
Mo1−C28	2.019(5)	O7−C29	1.159(5)
Mo1−C29	1.940(4)	O8−C30	1.154(5)
Mo1−C30	1.957(5)		
O1−Zr1−O4a	76.6(1)	C27−Mo1−C28	171.7(2)
O3a−Zr1−O4a	56.57(9)	C29−Mo1−C30	86.9(2)
O2−Mo1−S1	74.49(7)	O1−C23−O2	123.4(4)
S1−Mo1−C29	98.9(1)	O3−C26−O4	119.1(3)
O2−Mo1−C30	99.8(1)		

Scheme 4

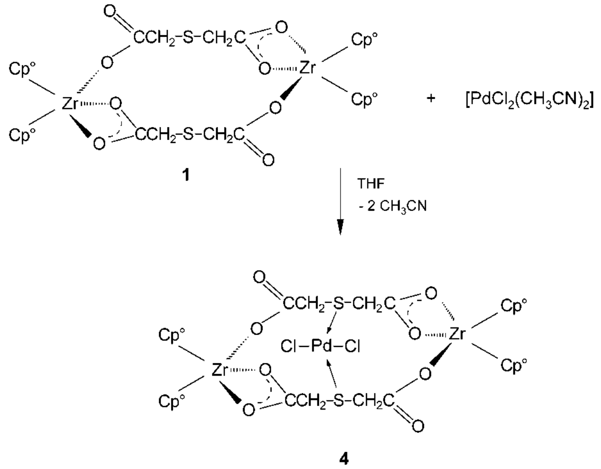

Scheme 5

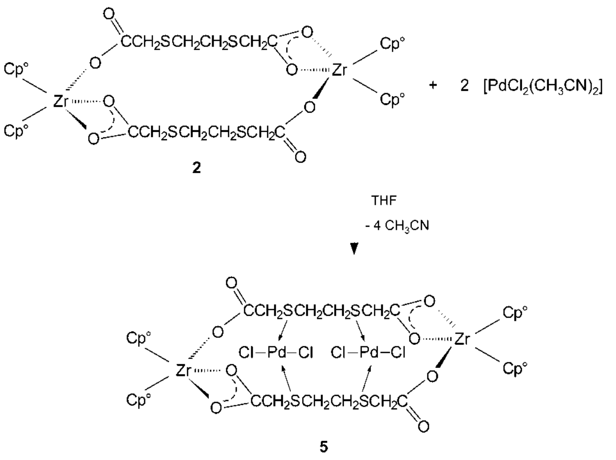

Mo1−C30 trans to S1, which are not significantly different. Thus, the oxygen atom appears to show a stronger trans influence here, similar to that of a sulfur atom, owing to the partial double-bond character of the O2−C23 bond. This effect was also observed for the published complexes described above. In the case of the tetranuclear Zr/Mo complex, we expected coordination of Mo to both sulfur donors. The observed coordination to one carboxylato oxygen atom and one sulfur donor may be sterically favored (formation of five-membered Mo−S−C−C−O rings), and the fact that Mo^0 is not a typical late (soft) metal center favors bonding to the hard oxygen donor.

Spectroscopic Studies on 3. In **3**, in which each molybdenum atom is coordinated to a carboxylato oxygen atom, the dynamic process described for **1** is stopped, as is reflected in the NMR data, even at room temperature. The ^{1}H NMR spectrum shows two broad downfield-shifted singlets for the CH_2 groups of the bridging ligands. However, the breadth of the signals indicates another dynamic process, in which probably the Mo−O bond is cleaved and a new Mo−O bond is formed to the oxygen atom of the second carboxylato group of the same ligand. This process is accompanied by a change in the bonding mode of the carboxylato group between mono- and bidentate, but it is slow enough for two signals to be observed rather than one averaged signal, as in **1**. In contrast to **1**, the Cp° ligands of one zirconocene fragment in **3** are now magnetically inequivalent, and this results in two sets of signals in the ^{1}H and $^{13}C\{^1H\}$ NMR spectra, which partly overlap.

Reaction of 1 and 2 with $[PdCl_2(CH_3CN)_2]$. The dimeric macrocyclic complex **1** reacts with 1 equiv of $[PdCl_2(CH_3CN)_2]$ to give a yellow solid in nearly quantitative yield, which is sparingly soluble in THF. Attempts to grow crystals from a CH_2Cl_2 solution at −20 °C led to decomposition of the product over 4 days. However, the NMR and IR data and the elemental analysis indicate the formation of the trinuclear Zr/Pd complex **4** (Scheme 4). Accordingly, the dimeric macrocyclic complex **2** reacts with 2 equiv of $[PdCl_2(CH_3CN)_2]$ to give **5** as a THF-soluble yellow solid in nearly quantitative yield. Using a molar ratio of 1:1 resulted in formation of the same product. Attempts to grow suitable crystals for an X-ray analysis failed, but on the basis of the elemental analysis we conclude that two $PdCl_2$ fragments are coordinated and therefore that a tetranuclear Zr/Pd complex was formed (Scheme 5).

Spectroscopic Studies on 4 and 5. In the IR spectrum of **4** and **5** the carboxylate vibrational bands are quite similar to those of the metalloligand **1** and **2**. This indicates the presence of mono- and bidentate bonding modes of the carboxylato groups in the solid state.

Table 4. Crystal Data and Data Collection Parameters

	1	2	3
formula	$C_{52}H_{76}O_8S_2Zr_2$	$C_{56}H_{84}O_8S_4Zr_2$	$C_{68}H_{92}Mo_2O_{18}S_2Zr_2$
M_r	1075.69	1195.91	1635.86
temp, K	223(2)	223(2)	223(2)
λ, Å	0.71073	0.71073	0.71073
cryst syst	monoclinic	triclinic	triclinic
space group	$P2_1/c$ (No. 14)	$P\bar{1}$ (No. 2)	$P\bar{1}$ (No. 2)
a, Å	17.1148(8)	9.012(2)	9.8376(14)
b, Å	9.3002(4)	9.454(2)	11.1310(16)
c, Å	32.6894(15)	17.750(4)	17.628(3)
α, deg	90	87.781(4)	99.365(2)
β, deg	103.5430(10)	83.709(4)	106.104(2)
γ, deg	90	71.316(4)	98.287(2)
V, Å^3	5058.5(4)	1423.9(4)	1792.9(4)
Z	4	1	1
density (calcd), mg/m^3	1.412	1.395	1.515
abs coeff, mm^{-1}	0.546	0.564	0.749
$F(000)$	2256	628	840
θ range, deg	1.22−27.05	1.15−28.29	1.23−29.07
no. of rflns collected	30 577	14 926	19 407
no. of indep rflns	10 971 (R_{int} = 0.0525)	6747 (R_{int} = 0.0828)	8607 (R_{int} = 0.0452)
refinement	full-matrix least squares on F^2		
no. of data/restraints/params	10 971/56/661	6747/1/320	8607/0/425
goodness of fit on F^2	0.971	1.093	0.992
final R indices ($I > 2\sigma(I)$)	R1 = 0.0376 wR2 = 0.0794	R1 = 0.1006 wR2 = 0.2665	R1 = 0.0451 wR2 = 0.0960
R indices (all data)	R1 = 0.0792 wR2 = 0.1051	R1 = 0.1439 wR2 = 0.2884	R1 = 0.0876 wR2 = 0.1139
largest diff peak and hole, e Å^{-3}	0.460/−0.434	2.041/−1.373	1.037/−0.738

The ^{1}H NMR spectrum of **4** shows an interesting coupling pattern. Thus, for the CH$_2$ protons two doublets with the same coupling constant of 15.4 Hz and a pronounced roof effect were observed. The ^{1}H,^{1}H COSY spectrum of **4** confirmed the assumption of a geminal coupling of the CH$_2$ protons. Furthermore, since one of the CH$_2$ signals is shifted downfield to 4.53 ppm, we assume formation of weak hydrogen bonds between the chloro ligands of the PdCl$_2$ fragment and one proton of each CH$_2$ group. In accordance with the observed magnetic inequivalence of the Cp° ligands (two sets of signals) and the ^{13}C{^{1}H} NMR spectrum we postulate a molecular structure in which the PdCl$_2$ fragment is coordinated to both sulfur donors and lies above the cavity of the molecule (see Scheme 4). In the ^{1}H NMR spectrum of **5** two doublets with a coupling constant of 16.8 Hz and two doublets with a coupling constant of 15.2 Hz were observed for the OOCCH$_2$ protons. In addition, both doublets show pronounced roof effects. Therefore, in analogy to **4** we assume geminal couplings of the OOCCH$_2$ protons, owing to weak hydrogen bonding to the chloro ligands of the PdCl$_2$ fragment. For the CH$_2$ protons of the ethylene bridge (SCH$_2$CH$_2$S) two multiplets were observed; that is, these protons are also magnetically inequivalent, so that geminal and vicinal couplings result. In contrast to **2** and **4** the ^{13}C{^{1}H} NMR spectrum of **5** shows two signals for the carboxylato carbon atoms at 184.5 and 170.1 ppm. This indicates that the dynamic process of the carboxylato groups is stopped here, even at room temperature, owing to the coordination of the two PdCl$_2$ fragments.

Summary

We have prepared a new class of macrocyclic zirconocene complexes containing oxygen and sulfur as donor atoms. These early-transition-metal macrocycles act as effective metalloligands for the coordination of a second metal. Further investigations on the complexation of other late transition metals and on catalytic properties of the prepared Zr/Mo and Zr/Pd complexes are in progress.

Experimental Section

General Details. All operations were carried out under a dry nitrogen atmosphere using standard Schlenk techniques. The reagents and solvents were purified by standard procedures. The ^{1}H and ^{13}C NMR spectra were recorded on a AVANCE DRX 400 spectrometer. The crystal structures were measured on a Siemens SMART CCD diffractometer. [Cp°$_2$ZrMe$_2$],[31] (HOOCCH$_2$SCH$_2$)$_2$,[32] [Mo(CO)$_4$(NBD)],[33] and [PdCl$_2$(CH$_3$CN)$_2$][34] were prepared by literature procedures. Thioglycolic acid was purchased from ACROS.

[Cp°$_2$Zr(OOCCH$_2$SCH$_2$COO)$_2$ZrCp°$_2$] (1). A solution of 0.3 g (2.0 mmol) of thioglycolic acid in 10 mL of THF was added to a solution of 0.84 g (2.0 mmol) of [Cp°$_2$ZrMe$_2$] in 10 mL of THF. The colorless solution was stirred overnight. Concentration of the solution to about half its volume and addition of 50 mL of petroleum ether gave a colorless precipitate of **1**. Suitable crystals for structure analysis were obtained from a concentrated THF solution of **1** at 4 °C. Yield: 0.81 g (75%). Mp: 275 °C dec. ^{1}H NMR (C$_6$D$_6$, 25 °C, 400 MHz): δ 3.58 (s, 8H, (OOCCH_2)$_2$S); 2.39 (q, $^3J_{HH}$ = 7.5 Hz, 8H, C$_5$Me$_4$CH_2CH$_3$); 1.88 (s, 24H, C$_5$Et(CH_3)$_4$); 1.82 (s, 24H, C$_5$Et(CH_3)$_4$); 0.84 (t, $^3J_{HH}$ = 7.5 Hz, 12H, C$_5$Me$_4$CH$_2$CH_3). ^{13}C{^{1}H} NMR (C$_6$D$_6$, 25 °C, 100.6 MHz): δ 179.0 (s, (OOCCH$_2$)$_2$S); 127.7, 122.8, 121.6 (s, C_5EtMe$_4$); 38.8 (s, (OOCCH$_2$)$_2$S); 20.0 (s, C$_5$Me$_4$$CH_2CH_3$); 15.1 (s, C$_5Me_4CH_2$$CH_3$); 11.8, 11.6 (s, C$_5$Et($CH_3$)$_4$). IR (KBr pellet): $\tilde{\nu}$ 1648 (C=O), 1535, 1334 (O−C−O), 1207 (C−O) cm^{-1}. ESI-MS (m/z, pos.): found, 1 075.315 70 [M + H$^+$]; calcd, 1 075.317 00 [M + H$^+$]. Anal. Calcd for $C_{52}H_{76}O_8S_2Zr_2$: C, 58.1; H, 7.1; S. 6.0. Found: C, 57.9; H, 7.1; S, 6.1.

[Cp°$_2$Zr(OOCCH$_2$SCH$_2$CH$_2$SCH$_2$COO)$_2$ZrCp°$_2$] (2). A solution of 0.36 g (1.7 mmol) of dithiotriglycolic acid in 10 mL of

---

(31) Threlkel, R. S.; Bercaw, J. E. *J. Organomet. Chem.* **1977**, *136*, 1.

(32) Ramberg, L.; Tiberg, A. *Chem. Ber.* **1914**, *47*, 730.

(33) Bauer, G. *Handbuch der anorganischen präparativen Chemie*; Ferdinand Enke Verlag: Stuttgart, Germany, 1981; Vol. 3, p 1884.

(34) Kharasch, M. S.; Seyler, R. C.; Mayo, F. R. *J. Am. Chem. Soc.* **1938**, *60*, 882.

THF was added to a solution of 0.72 g (1.7 mmol) of [Cp°$_2$ZrMe$_2$] in 10 mL of THF. The colorless reaction mixture was refluxed for 4 h and then cooled to room temperature. Concentration of the solution to about half its volume and addition of 50 mL of petroleum ether gave a colorless precipitate of **2** at −20 °C. Suitable crystals for structure analysis were obtained from a concentrated THF solution of **2** at 4 °C. Yield: 0.75 g (74%). Mp: 135−140 °C. ^{1}H NMR (CDCl$_3$, 25 °C, 400 MHz): δ 3.32 (s, 8H, $\mathrm{OOCC}H_2\mathrm{SCH}_2$); 3.01 (s, 8H, $\mathrm{OOCCH_2SC}H_2$); 2.32 (q, $^3J_{\mathrm{HH}} = 7.5$ Hz, 8H, $\mathrm{C_5Me_4C}H_2\mathrm{CH_3}$); 1.88 (s, 24H, $\mathrm{C_5Et(C}H_3)_4$); 1.87 (s, 24H, $\mathrm{C_5Et(C}H_3)_4$); 0.88 (t, $^3J_{\mathrm{HH}} = 7.5$ Hz, 12H, $\mathrm{C_5Me_4CH_2C}H_3$). ^{13}C{^{1}H} NMR (CDCl$_3$, 25 °C, 100.6 MHz): δ 178.8 (s, $\mathrm{OO}C\mathrm{CH_2SCH_2}$); 127.7, 122.7, 121.8 (s, $C_5\mathrm{EtMe_4}$); 37.1 (s, $\mathrm{OOC}C\mathrm{H_2SCH_2}$); 32.0 (s, $\mathrm{OOCCH_2S}C\mathrm{H_2}$); 19.6 (s, $\mathrm{C_5Me_4}C\mathrm{H_2CH_3}$); 14.9 (s, $\mathrm{C_5Me_4CH_2}C\mathrm{H_3}$); 11.7, 11.5 (s, $\mathrm{C_5Et(}C\mathrm{H_3)_4}$). IR (KBr pellet): $\tilde{\nu}$ 1635 (C═O), 1538, 1324 (O−C−O), 1205 (C−O) cm^{-1}. ESI-MS (m/z, pos.): found, 1 217.304 44 [M + Na$^+$]; calcd, 1 217.304 89 [M + Na$^+$]. Anal. Calcd for $\mathrm{C_{56}H_{84}O_8S_4Zr_2}$: C, 56.2; H, 7.1; S, 10.7. Found: C, 56.1; H, 6.6; S, 10.0.

3. A solution of 0.14 g (0.48 mmol) of [Mo(CO)$_4$(NBD)] in 10 mL of THF was added to a solution of 0.26 g (0.24 mmol) of **1** in 15 mL of toluene. The yellow reaction mixture was stirred for 4 h at room temperature. Addition of 40 mL of petroleum ether to the solution gave **3** as a crystalline, yellow solid. Suitable crystals for structure analysis were obtained from a concentrated THF solution at 4 °C. Yield: 0.21 g (66%). Mp: >300 °C. ^{1}H NMR (OC$_4$D$_8$, 25 °C, 400 MHz): δ 3.88 (br s, 4H, $\mathrm{(OOCC}H_2)_2\mathrm{S}$); 3.66 (br s, 4H, $\mathrm{(OOCC}H_2)_2\mathrm{S}$); 2.34 (m, $^3J_{\mathrm{HH}} = 7.2$ Hz, 8H, $\mathrm{C_5Me_4C}H_2\mathrm{CH_3}$); 1.92−1.88 (overlapping s, 48H, $\mathrm{C_5Et(C}H_3)_4$); 0.90 (m, 12H, $\mathrm{C_5Me_4CH_2C}H_3$). ^{13}C{^{1}H} NMR (OC$_4$D$_8$, 25 °C, 100.6 MHz): δ = 222.1, 219.1, 217.4 (s, OC-Mo); 182.0, 180.9 (s, $\mathrm{(OO}C\mathrm{CH_2)_2S}$); 129.0, 128.0, 123.8, 122.4, 121.7 (s, $C_5\mathrm{EtMe_4}$); 45.1, 38.9 (s, $\mathrm{(OOC}C\mathrm{H_2)_2S}$); 19.8, 19.7 (s, $\mathrm{C_5Me_4}C\mathrm{H_2CH_3}$); 14.1 (s, $\mathrm{C_5Me_4CH_2}C\mathrm{H_3}$); 11.25, 11.20, 10.8 (s, $\mathrm{C_5Et(}C\mathrm{H_3)_4}$). IR (KBr pellet): $\tilde{\nu}$ 2017, 1891, 1848 cm^{-1} (CO ligands), 1650 (C═O), 1533, 1334 (O−C−O), 1206 (C−O) cm^{-1}. Anal. Calcd for $\mathrm{C_{60}H_{76}Mo_2O_{16}S_2Zr_2}$: C, 48.3; H, 5.2; S, 4.3. Found: C, 47.9; H, 5.3; S, 4.2.

4. A solution of 0.16 g (0.15 mmol) of **1** in 10 mL of THF was added to a suspension of 0.04 g (0.15 mmol) of [PdCl$_2$(CH$_3$CN)$_2$] in 10 mL of THF. The yellow solution became clear, and after it was stirred for 1 h, a yellow precipitate of **4** formed, which was isolated and dried in vacuo. Yield: ca. 0.15 g (ca. 80%). Mp: >210 °C. ^{1}H NMR (CDCl$_3$, 25 °C, 400 MHz): δ 4.53 (d, $^2J_{\mathrm{HH}} = 15.4$ Hz, 4H, $\mathrm{(OOCC}H_2)_2\mathrm{S}$); 3.36 (d, $^2J_{\mathrm{HH}} = 15.4$ Hz, 4H, $\mathrm{(OOCC}H_2)_2\mathrm{S}$); 2.49 (q, $^3J_{\mathrm{HH}} = 7.6$ Hz, 4H, $\mathrm{C_5Me_4C}H_2\mathrm{CH_3}$); 2.42 (q, $^3J_{\mathrm{HH}} = 7.6$ Hz, 4H, $\mathrm{C_5Me_4C}H_2\mathrm{CH_3}$); 2.03 (s, 12H, $\mathrm{C_5Et(C}H_3)_4$); 2.01 (s, 12H, $\mathrm{C_5Et(C}H_3)_4$); 1.97 (s, 24H, $\mathrm{C_5Et(C}H_3)_4$); 0.90 (m, 12H, $\mathrm{C_5Me_4CH_2C}H_3$). ^{13}C{^{1}H} NMR (CDCl$_3$, 25 °C, 100.6 MHz): δ 172.1 (s, $\mathrm{(OO}C\mathrm{CH_2)_2S}$); 130.1, 129.8, 125.5, 124.5, 124.1, 123.4 (s, $C_5\mathrm{EtMe_4}$); 44.1 (s, $\mathrm{(OOC}C\mathrm{H_2)_2S}$); 19.9, 19.8 (s, $\mathrm{C_5Me_4}C\mathrm{H_2CH_3}$); 14.84, 14.80 (s, $\mathrm{C_5Me_4CH_2}C\mathrm{H_3}$); 12.2, 11.97, 11.92, 11.6 (s, $\mathrm{C_5Et(}C\mathrm{H_3)_4}$). IR (KBr pellet): $\tilde{\nu}$ 1651 (C═O), 1545, 1323 (O−C−O), 1206 (C−O) cm^{-1}. Anal. Calcd for $\mathrm{C_{52}H_{76}Cl_2O_8PdS_2Zr_2}$: C, 49.8; H, 6.07; O, 10.23; Cl, 5.66. Found: C, 48.9; H, 5.89; O, 10.91; Cl, 5.99.

5. A solution of 0.23 g (0.19 mmol) of **2** in 10 mL of THF was added to a suspension of 0.10 g (0.38 mmol) of [PdCl$_2$(CH$_3$CN)$_2$] in 10 mL of THF. The yellow solution became clear and was stirred for 1 h. Addition of 50 mL of petroleum ether gave an intense yellow precipitate at −20 °C, which was dried in vacuo. Yield: ca. 0.2 g (ca. 70%). Mp: 190−195 °C. ^{1}H NMR (CDCl$_3$, 25 °C, 400 MHz): δ 4.49 (d, $^2J_{\mathrm{HH}} = 16.8$ Hz, 2H, $\mathrm{OOCC}H_2\mathrm{SCH_2}$); 3.71 (d, $^2J_{\mathrm{HH}} = 16.8$ Hz, 2H, $\mathrm{OOCC}H_2\mathrm{SCH_2}$); 3.56 (m, 4H, $\mathrm{OOCCH_2SC}H_2$); 3.42 (m, 4H, $\mathrm{OOCCH_2SC}H_2$); 3.36 (d, $^2J_{\mathrm{HH}} = 15.2$ Hz, 2H, $\mathrm{OOCC}H_2\mathrm{SCH_2}$); 3.19 (d, $^2J_{\mathrm{HH}} = 15.2$ Hz, 2H, $\mathrm{OOCC}H_2\mathrm{SCH_2}$); 2.30 (m, 8H, $\mathrm{C_5Me_4C}H_2\mathrm{CH_3}$); 1.89−1.85 (overlapping s, 48H, $\mathrm{C_5Et(C}H_3)_4$); 0.87 (m, 12H, $\mathrm{C_5Me_4CH_2C}H_3$). ^{13}C{^{1}H} NMR (CDCl$_3$, 25 °C, 100.6 MHz): δ 184.5, 170.1 (s, $\mathrm{OO}C\mathrm{CH_2SCH_2}$); 128.2, 127.7, 123.6−121.6 (s partly overlapped, $C_5\mathrm{EtMe_4}$); 43.2, 39.5 (s, $\mathrm{OOC}C\mathrm{H_2SCH_2}$); 35.9, 34.6 (s, $\mathrm{OOCCH_2S}C\mathrm{H_2}$); 19.7 (br s, $\mathrm{C_5Me_4}C\mathrm{H_2CH_3}$); 14.9, 14.8 (s, $\mathrm{C_5Me_4CH_2}C\mathrm{H_3}$); 11.7−11.4 (overlapping s, $\mathrm{C_5Et(}C\mathrm{H_3)_4}$). IR (KBr pellet): $\tilde{\nu}$ 1651 (C═O), 1539, 1329 (O−C−O), 1209 (C−O) cm^{-1}. Anal. Calcd for $\mathrm{C_{56}H_{84}Cl_4O_8Pd_2S_4Zr_2}$: C, 43.4; H, 5.42; S, 8.26. Found: C, 44.5; H, 6.41; S, 8.53.

Supporting Information Available: Tables giving crystal structure data for **1**−**3** and figures giving ^{1}H and ^{13}C NMR spectra for **1**−**3**. This material is available free of charge via the Internet at http://pubs.acs.org.

OM0110336